Filtration and regeneration performances of SiC fiber potentially applied to gasoline particulates

by

Kazuhiro YAMAMOTO, Shinichi KONDO, Kazuya SUZUKI
Dep. Mechanical Systems Engineering, Nagoya University
Furo-cho, Chikusa-ku, Nagoya, Aichi 464-8603, JAPAN

Corresponding author: Kazuhiro Yamamoto
Dep. Mechanical Systems Engineering
Faculty of Engineering
Nagoya University
Furo-cho, Chikusa-ku, Nagoya, Aichi 464-8603, Japan
Tel: (+81)-52-789-4471, Fax: (+81)-52-789-4471
E-mail address: kazuhiro@mech.nagoya-u.ac.jp

Keywords: Filtration; Catalyst; Oxidation; SiC fiber; Pressure drop

Filtration and regeneration performances of SiC fiber potentially applied to gasoline particulates

by

Kazuhiro YAMAMOTO, Shinichi KONDO, Kazuya SUZUKI
Dep. Mechanical Systems Engineering, Nagoya University
Furo-cho, Chikusa-ku, Nagoya, Aichi 464-8603, JAPAN

ABSTRACT

In this study, for filtration of gasoline particulates, we tested SiC fibers potentially applied for a gasoline particulate filter (GPF). Carbon particles were used as model soot. Focusing on the porosity and the fiber diameter, the filtration efficiency and the pressure drop were examined. To promote the carbon oxidation, the fiber was coated with the Pt-catalyst. Results show that, by reducing the porosity, the filtration efficiency increases, but the pressure drop across the filter (filter backpressure) becomes larger. When the porosity is lower than 0.94, the improvement of filtration efficiency is not enough. Secondary, when the fiber with smaller diameter is adopted by keeping the porosity constant, the filtration efficiency is found to increase. Especially, the combination of 18, 14, 10 micrometer fiber sheets exhibits more efficient filtration performance without increasing the pressure drop. As for the continuous regenerating trap (CRT), the oxidation of carbon particles starts around 420 ºC, and more carbon particles are oxidized at higher temperature. At 600 ºC, the pressure drop can be kept smaller, because a part of deposited particles is continuously oxidized. At 800 ºC, the filtration efficiency is worsened with the larger pressure drop. From the above experimental data, the CRT at 600 ºC is suitable. When the fiber surface is coated with Pt catalyst, the oxidation of carbon particles starts at 250 ºC. When the temperature is higher than 330 ºC, the pressure drop of the catalyzed filter is even smaller than that of the non-catalyzed filter. It is concluded that the coating of catalysts is effective for reducing the pressure drop as well as the oxidation temperature.

1. Introduction

Particulate matters (PMs) including soot are a main source of air pollution, which could pose a major threat to our health and the climate change [1]. It has been confirmed that diesel exhaust is treated as one of the major sources of PM. Hence, authorities in many countries have introduced tighter emission standards based on the particle mass and the particle number [2,3], and a so-called diesel particulate filter (DPF) has been applied in the diesel exhaust after-treatment system [4-6].

On the other hand, in the case of the gasoline vehicles, the situation is rather complicated. In fact, in comparison with diesel vehicles, PM emissions from traditional port fuel injection (PFI) gasoline engines are known to be very low. However, especially in the European countries, gasoline direct injection (GDI) vehicles are expanding their share of the market on the grounds of better fuel efficiency [7]. The disadvantage is that GDI engines emit considerably more PM than PFI engines [8-10]. In light of more stringent regulations, some

automobile manufacturers have decided to equip modern gasoline vehicles with a gasoline particulate filter (GPF) [3, 11].

It is worth noting that there are several important characteristics of the gasoline exhaust, which could be different from those of the diesel exhaust. One is that the gasoline exhaust gas temperature is expectedly higher. Similar to DPF, GPF requires the frequent filter regeneration [12]. It should be noted that, during the regeneration, the diesel filter would be clacked or partially damaged in the presence of catalysts due to the sudden and/or unexpected temperature rise [13]. It may cause the irreversible damage to downstream after-treatment system components such as a well-known three way catalyst (TWC) [8,14]. Even in the case of diesel vehicles, the catalyzed DPF is widely used to reduce the regeneration temperature [15-17]. Similarly, we must avoid the damage of the gasoline after-treatment device due to the large temperature increase. That is, in view of durability, it may be inappropriate to oxidize the deposited soot in the filter at higher temperature

during the filter regeneration [18-20], because it causes the serious fuel penalty [10,13,15] as well as an additional risk of melting the filter [17]. Additionally, compared with the diesel soot, the particulate size from GDI is much smaller [2], and the number ratio of smaller particles is quite high in the gasoline exhaust. It may be difficult to attain enough filtration efficiency. From the above, an establishment of a new filtration system with enough thermal durability would be urgently required.

The focus of this work was an application of SiC fibers for the filtration system, which had been used for trapping diesel soot [20]. It could be potentially applied to GPFs. In our previous numerical simulation [21], we have reported that the porosity of SiC fiber can be increased up to 0.9, and the filter backpressure is expectedly low. Typically, in the case of the honeycomb filter, its porosity is lower than 0.6 [4,6,18,19]. Moreover, the SiC fiber has enough thermal durability. So far, any optimizations have not been conducted. One difficulty is that characteristics of gasoline particles unquestionably depend on fuel properties, exhaust

gas components, engine conditions, and driving cycles. Within the budget of time and resources, more laboratory results are needed for the system design in the light of fundamental knowledge of filtration and oxidation of the exhaust soot.

Here, in order to focus on non-volatile particles in the exhaust, we used carbon particles as model soot formed by a carbon particle generator [22]. The size distribution of particles is very stable and repeatable. If the conditions of nanoparticles in the feed gas are fixed, it would be much easier to optimize the filter properties such as the fiber diameter and the porosity [20,21]. Three fiber diameters of 10, 14, 18 μm were tested, and each fiber sheet was 1 mm thickness. To simulate a continuous regenerating trap, a tubular furnace was used, by which it was possible to control the mimic exhaust temperature [22]. To promote the carbon oxidation, the coating of Pt catalyst was newly tried [6,19,23].

2. Experimental setup

The filtration efficiency was evaluated by the measurement of the particle number concentration. The experimental setup during the filtration is shown in Fig. 1. The carbon particle generator was used to produce particles that were added to the mimic exhaust flow. To measure the pressure drop across the filter, corresponding to the filter backpressure, the pressure transmitter was used. One was connected to the flow pipe in front of the filter, and the other was set for detecting the atmospheric pressure. In the carbon oxidation experiments, the particles were oxidized by the temperature-programmed reaction (TPR) system equipped with the tubular furnace [21]. The temperature up to 1200 ºC could be set. The components of CO, CO_2 and O_2 were measured. The details are explained below.

2.1. Tubular furnace

To cause the oxidation of carbon particles at any fixed temperature, the electric tubular furnace, ARF-30MC (Asahi Rika Seisakusho Co. Ltd., Japan), was used [22], with a digital temperature controller, AMF-S (Asahi Rika Seisakusho Co. Ltd., Japan). The gas flow was heated with a temperature adjustment within the error of ± 2.5 ºC. For controlling the furnace temperature as well as for monitoring the filter inlet temperature, two thermocouples were used. It was confirmed that the temperature inside the furnace was quite uniform. In this experiment, the operating temperature was increased up to 820 ºC to simulate the continuous regenerating trap (CRT) system. This could be similar to the filtration combustion at constant temperature [24].

To flow the carbon particles in the mimic exhaust gas, a quartz reaction tube with an external diameter of 30 mm (internal diameter of 26 mm) and 560 mm length was inserted through the furnace, and the filter was set inside the quartz tube. The inflow velocity of 10 cm/s was given, which was the total flow rate divided

67 by the cross-sectional area of reaction tube. Considering the furnace length of 300 mm, the residence time was

68 3 s. The mole fraction of oxygen was set to be 10 % in the gas flow [25,26]. Since there might be no oxygen

69 in the stoichiometric gasoline exhaust, 10 % may be achieved by supplying an outer air to the exhaust.

70

71 *2.2. Carbon particle generator*

72 The carbon particle generator (DNP-2000; Palas GmbH, Germany) has been widely used in aerosol

73 science [27]. It can generate carbon particles having a fixed size distribution, which is suitable for laboratory

74 experiments [22]. The principle involves the use of two highly purified graphite rods as electrodes with a

75 discharge of 3000 V to generate nanoparticles. The particle concentration was controlled by changing the

76 discharge voltage. It produces the primary particles in the range of 20 to 300 nm, close to the real diesel or

77 gasoline soot [4,28]. The maximum of the particle feeding is the order of 10^7 1/cm^3.

78 *2.3. Measurement of particle size and gas component*

79 The particle size measurement system was composed of a dilution device (MD19-2E; Matter

80 Engineering AG, Switzerland), a high efficiency particulate air (HEPA) filter, a scanning mobility particle

81 sizer (SMPS3034; TSI Incorporated, USA) and a personal computer for data analysis. The sampling period of

82 SMPS was 3 min. To reduce the effect of static charge for minimizing particle loss along the tubing wall, the

83 conductive silicone tubing (TSI Incorporated) was used. The dilution device was needed to avoid the particle

84 aggregation. After preliminary tests for sampling, the dilution ratio by using the air was set to be 500:1 [22,29].

85 The gases of CO, CO_2 and O_2 were detected by an infrared gas analyzer (CGT-7000; Shimadzu Corporation,

86 Japan). The concentration accuracy was 1 ppm.

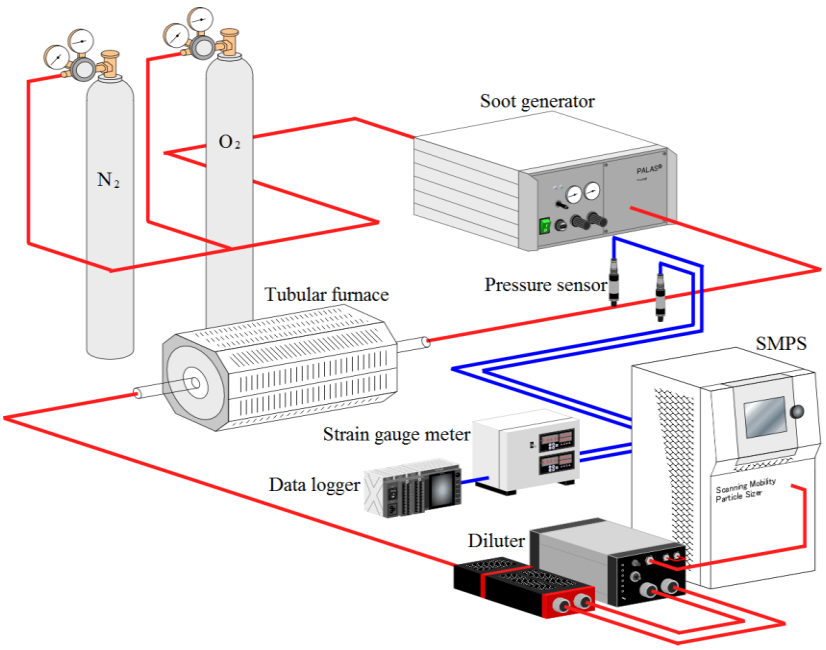

Fig. 1 Experimental setup for the particle size measurement during the filtration.

3. Results and discussion

3.1. Particle trap

Before evaluating the filtration performance, we observed the microscopic structure of fibers to see the change in appearance during the filtration. To monitor the deposition of carbon particles, three images of initial fiber together with those at the duration time of 30 and 90 min are shown in Fig. 2. These were

visualized by using a photomicrography of VK-9500 (Keyence Japan). The filtration test was conducted at room temperature, so that no particle oxidation occurred. In this figure, two sheets of 10 μm fiber diameter were used. Figure 2a shows the fiber structure before the particle deposition, showing the assembly of intertwined straight fibers. In Fig. 2b, the carbon particles adhered on the surface of fibers. When more particles were deposited in Fig. 2c, the thick layer of carbon particles was formed. The above deposition processes are called a depth filtration and a cake filtration, respectively [30].

Next, we measured the particle number concentration to evaluate the particle trap quantitatively. In this experiment, the temperature was also room temperature (25 ℃). Figure 3 shows the particle size distributions. Here, D_p is the so-called mobility diameter measured by SMPS. Two sheets of 10 μm fiber diameter were used. The size distribution of 0 min is the distribution at the filter inlet, and three distributions of 9, 21, 30 min of the duration time are shown. Gradually, as the time evolves, the particle number decreases.

After 9 min, the total particle number was reduced by half. During the filtration, the particle size distribution kept the similar shape, suggesting that the filtration efficiency could be independent on the particle size.

In terms of fiber properties, we focused on the porosity and the fiber diameter. First, the effect of the porosity was examined by changing the density of the fiber sheet. The true density of the fiber is 2.48 g/cm^3, and the number of fibers per unit volume was specifically varied by setting the different porosity. Expectedly, the better filtration efficiency would be achieved if the porosity of the filter is reduced, because the number of fibers for filtration is monotonically increased. The filtration efficiency is shown in Fig. 4a, together with the pressure drop (Δp) in Fig. 4b. Five different porosity of 0.92, 0.93, 0.94, 0.95 and 0.96 were tested, using two fiber sheets of 10 μm-diameter. In general, the porosity of the well-known wall-flow DPF is in the range from 0.4 to 0.6 [4-6]. The porosity of SiC fiber filter is much higher, and we can reduce the pressure drop easily.

Here, the filtration efficiency (f_N) is described by

$$f_N = \frac{\sum_i N_0(D_{pi}) - \sum_i N(D_{pi})}{\sum_i N_0(D_{pi})} \qquad (1)$$

where N_0 is the number of particles at the filter inlet, and N is the number of particles passing through the filter.

The above filtration efficiency is based on the particle number [4,6]. Its total error (variation) caused by the experimental variability such as the difference between samples and the time-variation in feeding particles would be within 10 %.

Independent of the porosity, as the duration time evolves, the filtration efficiency is improved, but the pressure drop also becomes larger. As seen in Fig. 2b, carbon particles are deposited along the fibers, with less spacing between fibers. Resultantly, the filtration efficiency becomes higher, but the pressure drop accordingly increases. As the porosity is lower, the filtration efficiency is increased, but the pressure drop becomes larger,

simply because it is difficult to pass the flow through the dense layer of deposited particles. However, in Fig. 4a, an insignificant improvement of filtration efficiency from the porosity of 0.95 and below is recognized. Further, in Fig. 4b, the pressure drop largely increases when the porosity is lower than 0.93. Then, the porosity of 0.94 could be more like a turning point. Afterwards, we set the porosity to be 0.94.

Next, effects of the fiber diameter were examined, which is shown in Fig. 5. Here, we used a set of three fiber sheets. First and second choices were three sheets with the same fiber diameter of 10 or 14 μm. The third choice was three different sheets, which was the combination of 18, 14, 10 μm-diameter sheets. Needless to say, when the porosity of each fiber sheet is the same, the number of fibers becomes smaller as the fiber diameter is larger. Thus, the sparse sheet of thick fibers was set more upstream, and conversely, the dense of thin fibers was set more downstream. It is seen that, under the constant porosity condition, the filtration efficiency of three 14 μm-diameter sheets is the worst, and that of three 10 μm-diameter sheets is the

139 best. Interestingly, the combination of 18, 14, 10 μm-diameter sheets almost exhibits the same filtration

140 efficiency as that of three 10 μm-diameter sheets, but the pressure drop is much smaller. Based on our

141 numerical simulation, it is found that, when the fiber sheet of the larger diameter is placed more upstream, the

142 deposition of carbon particles widely occurs inside the filter, resulting in the smaller pressure drop [21]. Then,

143 the combination of 18, 14, 10 μm fiber sheets is the best choice for the better filtration with the smaller

144 pressure drop.

145

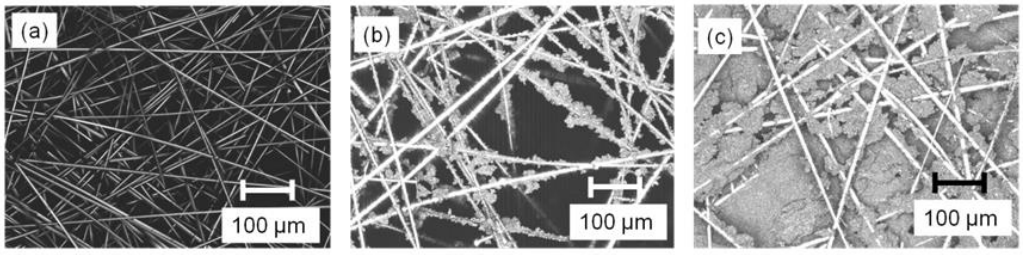

146

147 Fig. 2 Visualization of SiC fibers at the filtration time of (a) 0 min (b) 30 min (c) 90 min.

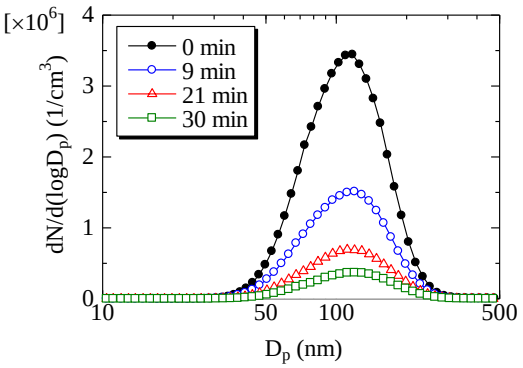

Fig. 3 Particle size distributions at 0, 9, 21, 30 min.

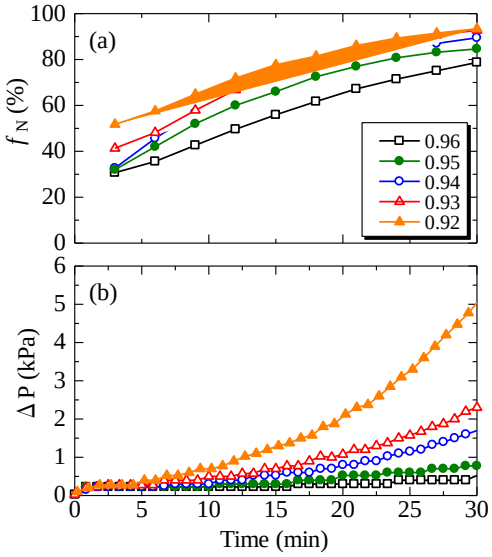

Fig. 4 (a) filtration efficiency and (b) pressure drop at different porosity.

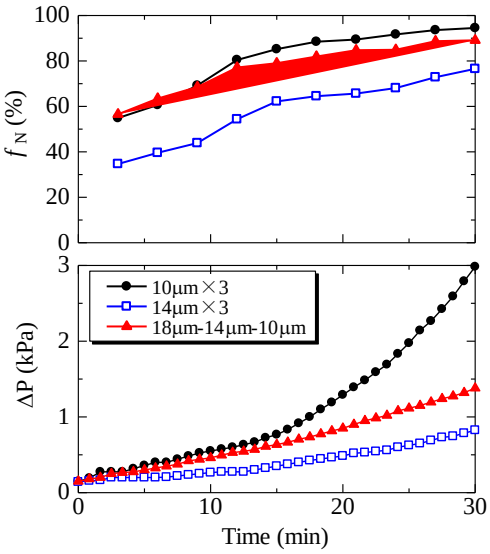

153

154 Fig. 5 (a) filtration efficiency and (b) pressure drop at different fiber diameter.

155

156 *3.2. Continuous regenerating trap (CRT)*

157 It is important to emphasize that the filter back-pressure must be kept at lower level, because the larger

158 back-pressure would increase the fuel consumption rate and decrease the available torque [3-7,18-20]. Then,

159 we need to oxidize the excessive deposited soot to avoid the larger pressure drop. Accordingly, a

160 comprehensive understanding of soot oxidation during the filter regeneration is required [31]. However, we

161 cannot observe the oxidation process directly, because most of particles are trapped by the filter. In order to
162 evaluate the variation of the size and their number concentration of trapped particles during the filter
163 regeneration, we firstly investigated the particle oxidation process without the filter.

164 Figure 6 shows the size distributions of carbon particles by setting the furnace temperatures of 25, 345,
165 422, 530, 660 and 820 ºC. Little change is observed until the temperature is 422 ºC. At 530 ºC, the size
166 distribution is only shifted to the smaller particle size, with the same particle number. At 660 ºC, the size
167 distribution is more shifted with fewer particles. At 820 ºC, the size distribution is largely shifted and the mode
168 particle size which is almost the peak diameter is reduced by more than 50%, compared to the original value
169 before the particle oxidation.

170 Since CO and CO_2 are produced by the oxidation of carbon particles, the amount of oxidized particles
171 are quantified based on these concentrations. Figure 7 shows the total concentration of CO and CO_2. The

172 volume fraction of carbon particles in the flow (ϕ_v) is also indicated. As seen in Fig. 6, at 422 or 530 ºC, only

173 the particle size is smaller, but the particle number is almost the same. Hence, for evaluating the carbon

174 oxidation, the volume fraction could be more suitable than the particle number. Obviously, concentrations of

175 CO and CO_2 become higher as the furnace temperature is increased, because more carbon particles are

176 oxidized. The temperature at which ϕ_v starts to decrease matches the temperature at which CO and CO_2 are

177 produced. Thus, it is concluded that the particle size starts to decrease around 420 ºC, and then, the particle

178 number subsequently decreases due to the complete oxidation.

179 Finally, the filtration at higher temperature was tested. The combination of 18, 14, 10 μm fiber

180 sheets was used. Controlling the inlet temperature of the filter, the filtration efficiency and the pressure drop

181 were monitored by feeding the carbon particles. This situation is similar to the continuous regenerating trap

182 (CRT) system [19,32]. By considering the fact that the particle size would firstly decrease before the particle

number reduction, it is better to adopt the filtration efficiency based on the particle mass. Here, the filtration efficiency (f_m) is described by

$$f_{\mathrm{m}} = \frac{\rho\sum_{\mathrm{i}} N_0(D_{\mathrm{p,i}})\cdot d_{\mathrm{i}}^3 - \rho\sum_{\mathrm{i}} N(D_{\mathrm{p,i}})\cdot d_{\mathrm{i}}^3}{\rho\sum_{\mathrm{i}} N_0(D_{\mathrm{p,i}})\cdot d_{\mathrm{i}}^3} \qquad (2)$$

where ρ is the true density of carbon particles (=1.8 g/cm^3). Four different inlet temperatures of 25 (room temperature), 500, 600, 800 ºC were given. The resultant filtration efficiency and the pressure drop are shown in Fig. 8. As already explained, no particle oxidation occurs at 25 ºC. At this temperature, the cake filtration with 100 % filtration efficiency is achieved at 90 min (see Fig. 2c). It is noted that, as seen in Fig. 7, the oxidation of carbon particles is greatly accelerated when the temperature is higher than 500 ºC.

In the CRT system, the particle filtration and the oxidation would occur simultaneously. Thus, in the

calculation of f_m, the particle which is neither oxidized nor trapped is counted for the leakage through the filter.

Intuitively, at higher temperature, it is expected that the filtration efficiency be better with the smaller pressure drop, because more particles are oxidized. However, up to 500 ºC, the pressure drop is even larger than that of 25 ºC, because the higher temperature enlarges the pressure drop due to the flow expansion. Interestingly, at 600 ºC, the pressure drop can be kept smaller, because a part of deposited particles is continuously oxidized. Simultaneously, in Fig. 8a, the filtration efficiency becomes 100 % at an earlier stage. This is because trapped particles play a role in the filtration, and the suitable deposition layer of particles is formed. Inversely, at 800 ºC or higher, the filtration efficiency is worsened with the larger pressure drop. Then, it is derived that the CRT at 600 ºC would be ideal condition where the 100 % filtration can be kept with the smaller pressure drop.

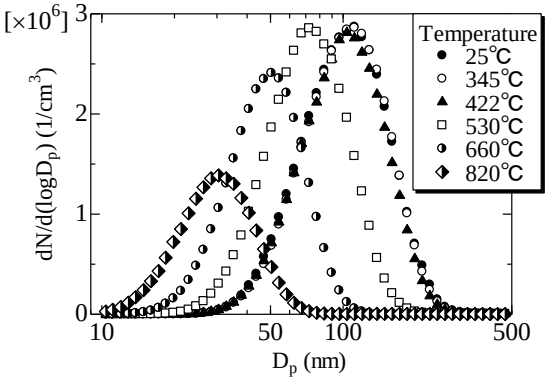

Fig. 6 Particle size distributions at different furnace temperature.

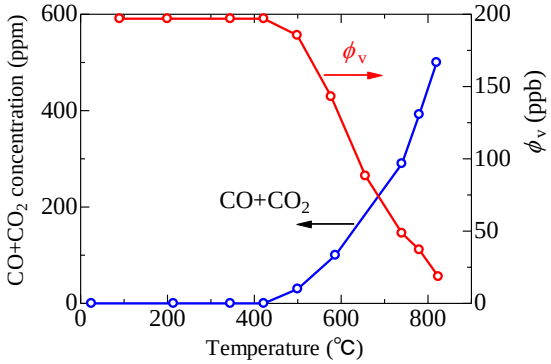

Fig. 7 Total concentrations of CO and CO_2 and volume fraction of carbon particles.

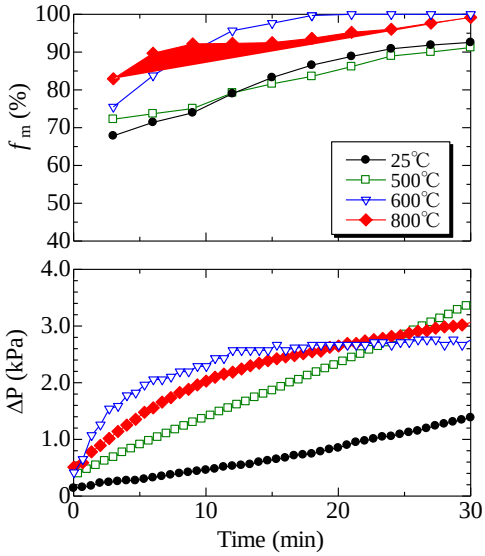

210

211 Fig. 8 (a) filtration efficiency and (b) pressure drop at different furnace temperature.

212

213 *3.3. Filter regeneration with catalysts*

214 In this section, the Pt-catalyzed filter was tested mainly for the reduction of oxidation temperature. In

215 experiments, the combination of 18, 14, 10 μm-diameter sheets was adopted. First, a Scanning Electron

216 Microscopy (S-3400N; Hitachi High-Technologies Corporation) coupled with EDX (X-Max; Oxford

217 Instruments) spectral data was applied to check the catalyst coating of the fiber. Figure 9 is the enlarged image

218 of 14 μm-diameter fiber, which was sampled from the fiber sheet. Unfortunately, when one fiber was taken, a

219 part of Pt-coating was peeled off. In this picture, two points were selected for the energy dispersive X-ray

220 spectroscopy. Point A shown by a filled circle was the Pt-coating layer, and point B shown by a triangle was

221 the detached area of the catalyst. The elements of C, O, Si and Pt were analyzed. The catalyst surface of point

222 A was mostly composed of Pt (93.5% Pt, 3.8% C, 0.7% O and 2.0% Si), in contrast to their weight percent of

223 point B: 3.1% Pt, 38.5% C, 5.9% O and 52.5% Si. It was confirmed that the fiber was successfully coated

224 with Pt-catalysts.

225 Then, the effect of catalysts on the filtration was examined. Figure 10 shows the filtration efficiency

226 and the pressure drop. The temperature was 25 ºC. One was the catalyzed filter, and the other was the

227 non-catalyzed filter. Both were composed of 18, 14, 10 μm-diameter sheets. As shown in Fig. 9, the catalyzed

228 fiber was thickened. Resultantly, there is less space between fibers, and the porosity was slightly reduced. As

229 seen in Fig. 10a, in the case of the catalyzed filter, the filtration efficiency is higher. It seems to be reasonable,

230 because the carbon particles would be easily trapped with narrow space between fibers. On the other hand, the

231 pressure drop of the catalyzed filter in Fig. 10b is increased.

232 Figure 11 shows the pressure drop of the filter composed of 18, 14, 10 μm-diameter sheets during

233 simple regeneration with and without catalysts. Initially, the same amount of carbon particles were deposited

234 inside both filters, corresponding to the conditions at t = 30 min in Fig. 10. At this point, the pressure drop of

235 the catalyzed filter was larger. Then, the temperature-programmed reaction (TPR) was started to evaluate the

236 effects of the catalyst on the carbon oxidation [8]. The heating rate was 10 ºC/min. At the beginning, by

237 increasing the temperature from 25 ºC, both pressure drops gradually increase due to the flow expansion. At

238 250 ºC, the pressure drop of the catalyzed filter starts to decrease, because carbon particles are oxidized by the

239 catalysts. Thus, from the view point of the pressure rise, the temperature of 250 ºC is a balanced point where

240 the negative effect of the flow expansion could be canceled by the positive effect of the carbon oxidation.

241 Afterwards, when the temperature is higher than 330 ºC, the pressure drop of the catalyzed filter is even

242 smaller than that of the non-catalyzed filter. It is seen that the pressure drop of the non-catalyzed filter turns to

243 decrease at 440 ºC, simply because the carbon oxidation starts around this temperature (see Fig. 7). We could

244 confirm that the coating of the catalysts is very effective for reducing the pressure drop as well as the oxidation

245 temperature.

246

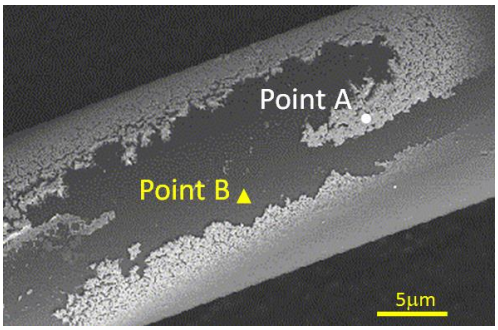

247

248 Fig. 9 SEM image of catalyzed SiC fiber of 14 μm is shown for energy dispersive X-ray spectroscopy.

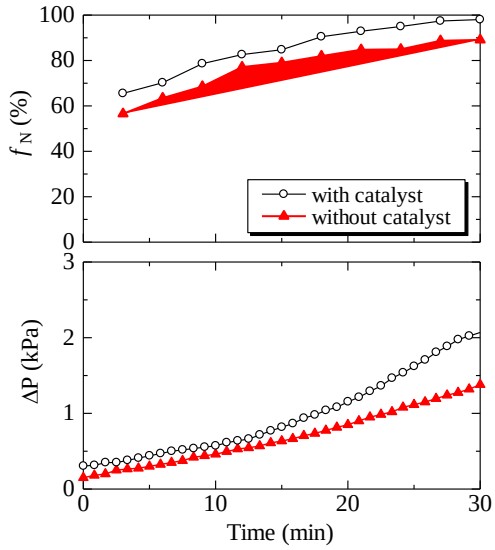

249

250 Fig. 10 (a) filtration efficiency and (b) pressure drop with and without catalyst at temperature of 25 ℃.

251

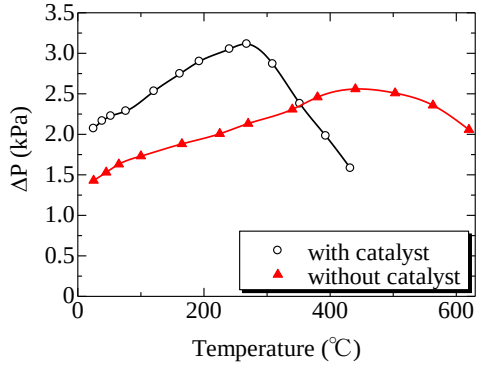

252

253 Fig. 11 Pressure drop during regeneration with and without catalyst.

254

4. Conclusions

In this work, the filter of SiC fibers was applied for exhaust gas filtration, by using carbon particles as model soot. Focusing on the porosity and the fiber diameter, the filtration efficiency and the pressure drop were examined. As for the filter regeneration, the inlet temperature of the filter was changed by the tubular furnace to simulate the continuous regenerating trap (CRT) as well as the simple oxidation of deposited particles. The following conclusions were derived:

(1) In the case of SiC fibers, particles are trapped by the depth filtration and the cake filtration. As the porosity of the filter is decreased, the filtration efficiency is higher, but the pressure drop becomes larger. When the porosity is lower than 0.94, the improvement of filtration efficiency is not enough. As the fiber diameter is reduced by keeping the porosity constant, the higher filtration efficiency is achieved, but the pressure drop accordingly increases. The combination of 18, 14, 10 μm-diameter sheets exhibits more efficient filtration

together with the smaller pressure drop.

(2) The oxidation of carbon particles starts around 420 ºC. At higher temperature, more particles are oxidized, but the pressure drop is larger, because the higher temperature enlarges the pressure drop due to the flow expansion. At 600 ºC, it is possible to reduce the pressure drop by keeping the 100 % filtration, because the desirable layer of deposited particles is formed. At 800 ºC or higher, the filtration efficiency is worsened with the larger pressure drop. Then, the CRT at 600 ºC is suitable.

(3) It was confirmed that the fiber was successfully coated with Pt-catalysts. When the temperature is relatively low, the pressure drop of the catalyzed filter is always larger because pores between fibers are partially plugged. At 250 ºC, the pressure drop of the catalyzed filter turns to decrease. When the temperature is higher than 330 ºC, the pressure drop of the catalyzed filter is even smaller than that of the non-catalyzed filter. Therefore, the coating of the catalysts is effective for reducing the pressure drop as

277 well as the oxidation temperature.

278

279 **References**

280 [1] Lawal AT. Polycyclic aromatic hydrocarbons. A review. Cogent Environmental Sci 2017; 3: 1-89.

281 [2] Mamakos A, Martini G, Marotta A, Manfredim U. Assessment of different technical options in reducing

282 particle emissions from gasoline direct injection vehicles. J Aerosol Sci 2013; 63:115-25.

283 [3] Johnson TV. Vehicular emissions in review. Technical Paper, 2017-01-0907; 2017.

284 [4] Tsuneyoshi K, Takagi O, Yamamoto K. Effects of washcoat on initial PM filtration efficiency and pressure

285 drop in SiC DPF. SAE Technical Paper, 2011-01-0817; 2011.

286 [5] Lapuerta M, Oliva F, Agudelo JR, Boehman AL. Effect of fuel on the soot nanostructure and

287 consequences on loading and regeneration of diesel particulate filters. Combust Flame 2012; 159:844-53.

288 [6] Tsuneyoshi K, Yamamoto K. Experimental study of hexagonal and square diesel particulate filters under
289 controlled and uncontrolled catalyzed regeneration. Energy 2013; 60:325-32.
290 [7] Spiess S, Wong KF, Richter JM, Klingmann R. Investigations of emission control systems for gasoline
291 direct injection engines with a focus on removal of particulate emissions. Top Catal 2013; 56:434-39.
292 [8] Überall A, Otte R, Eilts P, Krahl J. A literature research about particle emissions from engines with direct
293 gasoline injection and the potential to reduce these emissions. Fuel; 2015; 147:203-07.
294 [9] Wang Y, Zheng R, Qin Y, Peng J, Li M, Lei J, Wu Y, Hu M, Shuai S. The impact of fuel compositions on
295 the particulate emissions of direct injection gasoline engine. Fuel; 2016; 166:543-52.
296 [10] Jin D, Choi K, Myung CL, Lim Y, Lee J, Park S. The impact of various ethanol-gasoline blends on
297 particulates and unregulated gaseous emissions characteristics from a spark ignition direct injection (SIDI)
298 passenger vehicle. Fuel; 2017; 209:702-12.

299 [11] Yu L, Shuai S, Li Y, Li B, Liu H, He X, Wang Z. An experimental investigation on thermal efficiency of
300 a compression ignition engine fueled with five gasoline-like fuels. Fuel; 2017; 207:56-63.
301 [12] Gerardo DJ, Guerrero P, Yousef AH, Abhijeet R, Samuel S, Tharalekshmy A, Vaithilingam B. On the
302 characteristics and reactivity of soot particles from ethanol-gasoline and 2,5-dimethylfuran-gasoline
303 blends. Fuel; 2018; 222:42-55.
304 [13] Abián M, Martín C, Nogueras P, S-Valdepeñas S, R-Fernández J, Lapuerta M, Alzueta MU. Interaction
305 of diesel engine soot with NO_2 and O_2 at diesel exhaust conditions. Effect of fuel and engine operation
306 mode. Fuel; 2018; 242:455-61.
307 [14] Chen L, Liang Z, Zhang X, Shuai, S. Characterizing particulate matter emissions from GDI and PFI
308 vehicles under transient and cold start conditions. Fuel; 2017; 189:131-40.
309 [15] Schejbal M, Šteˇpánek J, Marek M, Kocˇí P, Kubícˇek M. Modelling of soot oxidation by NO_2 in various

types of diesel particulate filters. Fuel; 2010; 89:2365-75.

[16] Palma V, Ciambelli P, Meloni E, Sin A. Catalytic DPF microwave assisted active regeneration. Fuel; 2015; 140:50-61.

[17] Soltani S, Andersson R, Andersson B. The effect of exhaust gas composition on the kinetics of soot oxidation and diesel particulate filter regeneration. Fuel; 2018; 220:453-63.

[18] Yamamoto K, Oohori S, Yamashita H, Daido S. Simulation on soot deposition and combustion in diesel particulate filter. Proc Combust Inst 2009; 32:1965-72.

[19] Yamamoto K, Yamauchi K. Numerical simulation of continuously regenerating diesel particulate filter. Proc Combust Inst 2013; 34:3083-90.

[20] Yamamoto K, Fujikake F, Matsui K. Non-catalytic after-treatment for diesel particulates using carbon-fiber filter and experimental validation. Proc Combust Inst 2013; 34:2865-75.

321 [21] Yamamoto K, Toda Y. Numerical study on filtration of soot particulates in gasoline exhaust gas by SiC
322 fiber filter. Key Engineering Materials 2013; 735:119-26.
323 [22] Yamamoto K, Kanamori Y. Measurements of size distribution and oxidation rate of PM with NO_2. SAE
324 Technical Paper, 2015-01-1995; 2015.
325 [23] Yamamoto K, Sakai T. Simulation of continuously regenerating trap with catalyzed DPF. Catalysis
326 Today 2015; 242:357-62.
327 [24] Lutsenko NA. Modeling of heterogeneous combustion in porous media under free convection. Proc
328 Combust Inst 2013; 34:2289-94.
329 [25] Uchisawa J, Obuchi A, Ogata A, Enomoto R, Kushiyama S. Effect of feed gas composition on the rate of
330 carbon oxidation with Pt/SiO_2 and the oxidation mechanism. Applied Catalysis B 1999; 21:9-17.
331 [26] Wu X, Lin F, Wang L, Weng D, Zhou Z. Preparation methods and thermal stability of Ba-Mn-Ce oxide

catalyst for NOx-assisted soot oxidation. J. Environmental Sci. 2011; 23:1205-10.

[27] Evans DE, Harrison RM, Ayres JG. The generation and characterisation of elemental carbon aerosol for human challenge studies. Aerosol Science 2003; 34:1023-41.

[28] Kittelson DB. Engines and nanoparticles: A review. J Aerosol Sci 1998; 29: 575–88.

[29] Fennell PS, Dennis JS, Hayhurst AN, The sampling of nanoparticles of MgO formed when doping an oxygen-rich flame with magnesium: The measurement of the concentrations and size-distributions of these nanoparticles. Combust Flame 2007; 151:560-72.

[30] Barhate RS, Sundarrajan S, Pliszka D, Ramakrishna S. Fine chemical processing: The potential of nanofibres in filtration. Filtration & Separation 2008; 45:32-35.

[31] Lee KO, Seong H, Choi SM. Detailed analysis of kinetic reactions in soot oxidation by simulated diesel exhaust emissions. Proc Combust Inst 2013; 34:3057-65.

343 [32] Lizarraga L, Souentie S, Boreave A, George C, D'Anna B, Vernoux P. Effect of diesel oxidation catalysts

344 on the diesel particulate filter regeneration process. Environmental Sci Tech 2011; 45:10591-97.